Synthesis and Characterization of Poly(3-Sulfopropylmethacrylate) Brushes for Potential Antibacterial Applications

Madeleine Ramstedt,*,†,£ Nan Cheng,† Omar Azzaroni,† Dimitris Mossialos,‡,§ Hans Jörg Mathieu,£ and Wilhelm T. S. Huck*,†

Melville Laboratory for Polymer Synthesis, Department of Chemistry, University of Cambridge, Lensfield Road, Cambridge, CB2 1EW, UK, Department of Fundamental Microbiology, University of Lausanne (UNIL), CH-1015 Lausanne, Switzerland, Department of Biochemistry and Biotechnology, University of Thessaly, GR-41221 Larissa, Greece, and Material Science, Ecole Polytechnique Fédérale de Lausanne (EPFL), Station 12, CH-1015, Lausanne, Switzerland

Received September 12, 2006. In Final Form: December 20, 2006

This article describes the aqueous atom transfer radical polymerization synthesis of poly(3-sulfopropylmethacrylate) brushes onto gold and Si/SiO$_2$ surfaces in a controlled manner. The effect of Cu(I)/Cu(II) ratio was examined, and a quartz crystal microbalance was used to study the kinetics of the brush synthesis. The synthesized brushes displayed a thickness from a few nanometers to several hundred nanometers and were characterized using atomic force microscopy, ellipsometry, Fourier transform infrared spectroscopy (FTIR), contact angle measurements, and X-ray photoelectron spectroscopy (XPS). The as-synthesized sulfonate brushes had very good ion-exchange properties for the ions tested in this study, i.e., Na$^+$, K$^+$, Cu^{2+}, and Ag$^+$. FTIR and XPS show that the metal ions are coordinating to sulfonate moieties inside the brushes. The brushes were easily loaded with silver ions, and the effect of silver ion concentration on silver loading of the brush was examined. The silver-loaded brushes were shown to be antibacterial toward both gram negative and gram positive bacteria. The silver leaching was studied through leaching experiments into water, NaNO$_3$, and NaCl (physiological medium). The results from these leaching experiments are compared and discussed in the article.

Introduction

In many sectors of our society there exists a need for antibacterial surfaces. One of the most obvious areas is in the healthcare sector where bacterial infections of implants and medical devices cause increased suffering, prolonged hospital visits, rejections of transplants, recurrent operations, and sometimes even death.[1,2]

The antibacterial properties of silver have been known for centuries, and silver (in a variety of forms) has emerged as a very efficient bactericide due to its efficiency and low toxicity to humans.[3] Silver is antibacterial through a combination of several processes. Silver ions forms bonds to, e.g., DNA and to the surface of bacterial membrane proteins, thereby influencing a multitude of different cell functions. This multi-action makes it difficult for bacteria to develop resistance toward silver and, furthermore, to transfer such resistance between bacterial strains.[4–5] Many examples of antibacterial surfaces containing silver have been described in the literature in the form of silver nanoparticles,[6,7] silver halide salts,[8,9] or silver ions[10,11] in different organic matrices.

Polymer brushes consist of polymer chains that are tethered to a surface at sufficiently high grafting densities to force the polymer chains to exhibit a stretched confirmation that is rarely found in bulk polymers.[12] By growing brushes from the surface ("grafting from"), a higher density of polymer chains per surface area can be achieved compared to when polymers are grafted onto a surface ("grafting to").[13] In combination with a 'living' polymerization, polymer brushes with well-defined lengths, grafting densities, and composition can be obtained. Polyelectrolyte brushes are constructed from monomers carrying either positively or negatively charged functional groups. These films are very useful for ion exchange or to trap counter ions within the brush structure. The film properties depend on a large variety of factors such as fraction of dissociated ionic groups in the brush and salt concentration in the surrounding solution.[14] When a polyelectrolyte brush is collapsed in salt solution, excess electrolyte ions from solution get trapped inside the brush, and these can subsequently be leached out by repeated rinsing.[15] Brushes carrying functional groups such as phosphate, sulfonate, and carboxylate groups will display different properties depending on the pH of the surrounding fluid as a result of protonation of

* To whom correspondence should be addressed. Phone: +447784716633 (M.R.); +441223334370 (W.T.S.H.). E-mail: kmr48@cam.ac.uk (M.R.); wtsh2@cam.ac.uk (W.T.S.H.).

† University of Cambridge.
‡ University of Lausanne.
§ University of Thessaly.
£ Ecole Polytechnique Fédérale de Laussanne.

(1) Rimondini, L.; Fini, M.; Giardino, R. *J. Appl. Biomater. Biomech.* **2005,** *3,* 1–10.
(2) Campoccia, D.; Montanaro, L.; Arciola, C. R. *Biomaterials* **2006,** *27,* 2331–2339.
(3) Melaiye, A.; Youngs, W. J. *Expert Opin. Ther. Pat.* **2005,** *15,* 125–130.
(4) Percival, S. L.; Bowler, P. G.; Russel, D. J. *Hosp. Infect.* **2005,** *60,* 1–7.
(5) Modak, S. M.; Fox, C. L. Jr. *Biochem. Pharmacol.* **1973,** *22,* 2391–2404.

(6) Davenas, J.; Thévenard, P.; Philippe, F.; Arnaud, M. N. *Biomol. Eng.* **2002,** *19,* 263–268.
(7) Morones, J. R.; Elechiguerra, J. L.; Camacho, A.; Holt, K.; Kouri, J.B.; Ramirez, J. T.; Yacaman, M. J. *Nanotechnology* **2005,** *16,* 2346–2353.
(8) Sambhy, V.; MacBride, M.; Peterson, B. R.; Sen, A. *J. Am. Chem. Soc.* **2006,** *128,* 9798–9808.
(9) Adams, A. P.; Santschi, E. M.; Mellencamp, M. A. *Vet. Surg.* **1999,** *28,* 219–225.
(10) Shi, Z.; Neoh, K. G.; Zhong, S. P.; Yung, L. Y. L.; Kang, E. T.; Wang, W. *J. Biomed. Mater. Res.* **2005,** *76A,* 826–834.
(11) Ramstedt, M.; Houriet, R.; Mosialos, D.; Haas, D.; Mathieu, H. J. Wet chemical silver treatment of endotracheal tubes in order to produce antibacterial surfaces, manuscript submitted to *J. Biomed. Mater. Res. B,* in press, 2007.
(12) Jones, A. L.; Richards, R. W. *Polymers at Surfaces and Interfaces;* Cambridge University Press: New York, 1999.
(13) Zhao, B.; Brittain, W. J. *Prog. Polym. Sci.* **2000,** *25,* 677–710.
(14) Dobrynin, A. V.; Rubinstein, M. *Prog. Polym. Sci.* **2005,** 1049–1118.
(15) Azzaroni, O.; Moya, S.; Farhan, T.; Brown, A. A.; Huck, W. T. S. *Macromolecules* **2005,** *38,* 10192–10199.

functional groups.[16,17] These so-called "weak" polyelectrolyte brushes exhibit very interesting characteristics for many different types of applications using ion exchange. Examples of applications are "switching surfaces"[16] or usage as ink nanoreservoirs for microcontact printing.[18] Polyanionic polymer brushes can act as a reservoir for cations, such as silver ions, that subsequently can be released into surrounding fluids in a more or less controlled manner.

The great advantage of polymer brushes over, e.g., spin-coated layers of polymer is the enhanced accessibility between the functional groups and the aqueous solution given by the stretched confirmation in polymer brushes. In this way, substances from solution can interact more freely with functional groups on the brush compared to functionalities inside a polymer deposited onto a surface. Atom transfer radical polymerization (ATRP) is a simple, robust, and effective method of rapid polymer synthesis under easily controllable reaction conditions.[19] Using ATRP, polyelectrolyte brushes can be grown on surfaces with all types of geometry and the thickness of the surface film can be controlled from a few nanometers to several hundred. Another advantage of ATRP is the high degree of control over the polymerization reaction leading to the synthesis of polymer chains with low polydispersity. In the case of surface-initiated ATRP, this is observed in the synthesis of smooth polyelectrolyte films covalently anchored to the substrate. By modifying the structure of the anchoring part of the initiator molecule, polyelectrolyte brushes can be grown a large variety of surfaces including polymers[20] and inorganic material (such as glass).[21,22] Due to the covalent bonding between the substrate and the surface layer, these brushes are also expected to form a more robust surface layer compared to precipitates or polymers composites that are just deposited onto a surface.[23]

The objective of this research was to, in a controlled manner, synthesize anionic polyelectrolyte brushes bearing sulfonate groups and to use these to trap silver ions inside the polyelectrolyte films. In this way, we aimed at creating an antibacterial surface that also slowly leached therapeutic concentrations of silver ions into the surroundings.

Experimental Section

Chemicals. All chemicals were analytical reagent grade and were used as received from the manufacturer unless stated otherwise. 3-Sulfopropylmethacrylate (98%) (SPM) in the form of a potassium salt was obtained from Sigma-Aldrich, as was sodium chloride, sodium nitrate, copper (II) chloride (97%) ($Cu(II)Cl_2$), copper(I) chloride (99.995+%) ($Cu(I)Cl$), and 2,2′-bipyridyl (99+%) (BiPy). $Cu(I)Cl$ was stored under vacuum until needed. KNO_3 and $AgNO_3$ were obtained from Fluka and BDH. Solvents used were obtained from Fisher (ethanol, methanol, and acetone) and Tim Llayt (toluene, subsequently dried and distilled). Deionized water with a resistance of 18.2 MΩ·cm was obtained from a Millipore Simplicity 185 system. Triethylamine (Lancaster) was distilled and stored over KOH before use. Silicon wafers (Compart Technology Ltd, 100 mm diameter, boron-doped ⟨1 0 0⟩ orientation, one side polished) were cleaned using an Emitech K1050X plasma asher in dry air plasma mode, 100 W for 10 min prior to use.

Instrumentation. Ellipsometer measurements were carried out using a DRE ELX-02C ellipsometer with a 632.8 nm laser at 70°

from the normal. Refractive indices of 1.45 were used for initiator and polymer layers. Six points on each sample were analyzed and averaged.

Contact angle goniometry was performed using a homemade stage with a computer-controlled microsyringe and a digital camera. Infusion and withdrawal rates of 1 μL/min were used, and images for advancing and receding angles were recorded.

Fourier transform infrared spectroscopy (FTIR) measurements were performed on a BioRad spectrometer in transmission mode with a resolution of 4 cm^{-1} and 256 scans for each spectrum. The sample compartment was carefully purged with nitrogen to reduce any interference of water and carbon dioxide absorption from the gas phase.

X-ray photoelectron spectroscopy (XPS) analyses were performed using a Kratos Axis Ultra under monochromatic Al Kα radiation (1486.6 eV). A pass energy of 80 eV and a step size of 1 eV were used for survey spectra. For high-energy resolution spectra of regions, a pass energy of 20 eV and a step size of 0.1 eV were used. Charging neutralizing equipment was used to compensate sample charging, and the binding scale was referenced to the CH component of C 1s spectra at 285.0 eV. The concentrations obtained ($<\pm10\%$) are reported as the percentage of that particular atom species (at %) at the surface of the sample (<10 nm analysis depth).[24] To determine the elemental state of silver, a Wagner plot for chemical states was constructed using the kinetic energy for the Ag auger (M^4NN) peak, as well as the binding energy for the Ag $3d^{5/2}$ peak as previously described.[11] The position of the data in this plot indicated that silver is present in ionic form in the sulfonate brush.

Atomic force microscopy (AFM) measurements were performed on a Pico SPM (Molecular Imaging (MI)) in tapping mode. Cantilevers (Type II MAC levers) with a force constant of ∼2.8 N/m and a thickness of 3 μm were used for imaging. Imaging was performed on dry samples and roughness was calculated using the software provided by MI.

Quartz crystal microbalance (QCM) measurements were performed on a Q-Sense (Gothenburg, Sweden). The balance is equipped with a cell which is closed on one side by the quartz crystal. The flux of fluid into and through the cell was controlled by the standard Q-Sense flow system. The quartz crystals, purchased from Q-Sense, have a main resonance frequency of 5 MHz.

X-ray powder diffraction (XRD) measurements were performed on a Siemens Kristalloflex 805 equipped with a Cu tube. The diffraction patterns were collected from 5° up to 80° at a step size of 0.04 and 2 s per step.

Optical microscopy was done on a Nikon Eclipse ME600L microscope equipped with a Nikon Dn100 digital net camera.

Analyses of silver concentrations were performed using ICP by a commercial lab for water analysis (Eclipse Scientific Group in Ashford, Kent, UK).

Brush Preparation. Brushes were grown on both Si/SiO_2 and Au. Thick sulfonate brushes were grown on Si/SiO_2 functionalized with a monolayer of 2-bromo-2-methyl-propionic acid 3-trichlorosilanyl-propyl ester. The synthesis of the ester silane initiator and monolayer deposition onto the silicone wafer was performed as previously described by Brown et al.[25] The polymerizations were carried out using aqueous ATRP: 17.29 g of the sulfonate monomer (3-sulfopropylmethacrylate) was dissolved by stirring in 20 mL of methanol and 10 mL of water at room temperature (20 °C). To this solution 0.651 g of BiPy and 0.0114 g of $Cu(II)Cl_2$ were added. The mixture was stirred and degassed by $N_2(g)$ bubbling for an hour before 0.1648 g of $Cu(I)Cl$ was added. The mixture (still with $N_2(g)$ bubbling) was left for 15 min. Initiator-coated silicon wafer samples were sealed in a Schlenk tube and degassed (4 × high vacuum pump/N_2 refill cycles). The reaction mixture was syringed into this Schlenk tube, adding enough to cover the sample completely, and the mixture was left overnight under $N_2(g)$. The following day the

(16) Zhou, F.; Huck, W. T. S. *Chem. Commun.* **2005**, 5999−6001.

(17) Konradi, R.; Rühe, J. *Macromolecules* **2004**, *37*, 6954−6961.

(18) Azzaroni, O.; Moya, S. E.; Brown, A. A.; Zheng, Z.; Donath, E.; Huck, W. T. S. *Adv. Funct. Mater.* **2006**, *16*, 1037−1042.

(19) Matyjaszewski, K. *Macromolecules* **1998**, *31*, 4710−4717.

(20) Farhan, T. Huck, W. T. S. *Eur. Polym. J.* **2004**, *40*, 1599−1604.

(21) Ejaz, M.; Tsujii, Y.; Fukuda, T. *Polymer* **2001**, *42*, 6811−6815.

(22) Hamelinck, P. J.; Huck, W. T. S. *J. Mater. Chem.* **2005**, *15*, 381−385.

(23) Azzaroni, O.; Zheng, Z.; Yang, Z.; Huck, W. T. S. *Langmuir* **2006**, *22*, 6730−6733.

(24) Ratner, B. D.; Castner, D. G. In *Surface Analyses−The Principal Techniques*; Vickerman, J. C., Ed.; Wiley and Sons: Chichester, UK, 1997; Chapter 3.

(25) Brown, A. A.; Khan, N. S.; Steinbock, L.; Huck, W. T. S. *Eur. Polym. J.* **2005**, *41*, 1757−1765.
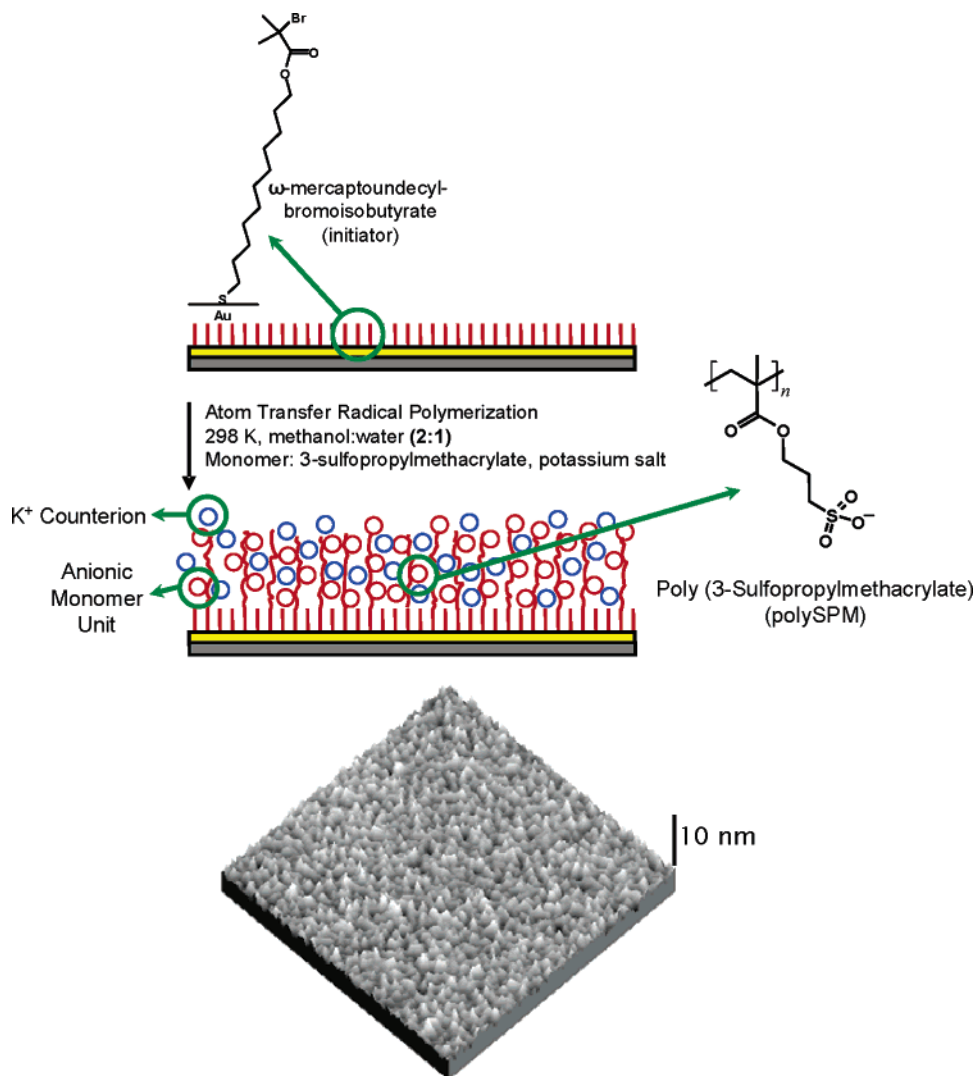
Figure 1. Schematic description of the synthesis of polySPM (sulfonate brush) and atomic force microscopy image showing the surface of a 210 nm thick polySPM brush grown on gold substrate. The scale bar represents 10 nm, and the scanned area is $5 \times 5 \ \mu m^2$ large. Surface roughness over this area was 1.45 nm.

samples were removed and thoroughly rinsed with deionized water and dried under a stream of $N_2(g)$. This gave rise to a brush thickness of around 300 nm.

Polyelectrolyte brushes on Au were used to study the kinetics of brush growth and for AFM studies. Syntheses of brushes from Au surfaces were carried out using a thiol initiator, ω-mercaptoundecyl bromobutyrate. Gold-coated wafers were immersed into 5 mM initiator solution overnight. The polymerization solution was prepared by dissolving 34.58 g of sulfonate monomer in 20 mL water and 40 mL methanol as above. $CuCl_2$ was added, and the solution degassed for 20 min. Thereafter, 0.3296 g of CuCl was added and the solution was degassed for 30 more minutes. The different ratios between Cu(I) and Cu(II) were obtained by varying the amount of $CuCl_2$. Molar ratios of 4.38, 3.4, 2.95, 2.72, 2.27, 2.04, 1.98, and 0.58 were prepared. Samples were removed after various polymerization times and washed with water and methanol several times.

To study the uptake of metal ions, thick brushes (around 300 nm) were immersed in different solutions containing 100 mM of Ag^+, K^+, or Cu^{2+} or $1 \ \mu M-1$ M Ag^+ for 24 h or overnight. For silver-leaching experiments, samples were soaked in 100 mM Ag^+ for 24 h to ensure good uptake of silver ions, dried under a stream of $N_2(g)$, and subsequently immersed into 5 mL of distilled water for 1 h. After the hour, the samples were taken up, the first sample was dried under $N_2(g)$, and the others immersed into 5 mL aliquots of fresh distilled water, this procedure was repeated until the last sample had been immersed in a total of 30 mL and 6 h. The solutions were analyzed for content of silver and the sample surfaces analyzed

using FTIR, XPS, and ellipsometry. Leaching experiments into 150 mM NaCl and 150 mM $NaNO_3$ solutions were performed in the same way but using a chosen salt solution instead of distilled water.

Bacterial Growth Assays. Bacterial growth tests were performed according to the method of Tiller et al.[26] A liquid culture (10 mL) of *Pseudomonas aeruginosa* wild type (PAO1), in exponential growth phase (OD_{600} 0.4−0.6), was centrifuged, washed with sterile water, centrifuged, and resuspended in 10 mL of sterile water. The samples were sprayed with *P. aeruginosa* in a fume hood. They were deposited onto a clean culture dish, left to dry slightly for 1−2 min, and covered with Luria Broth agar (LB agar, Difco, ∼20 mL) containing 1% KNO_3. The dishes were incubated overnight at 37 °C. Replicas of three were done for each sample. The same procedure was used for *Staphylococcus aureus* but without KNO_3 and using tryptic soy agar (Difco).

Results and Discussion

Synthesis of Polyelectrolyte Brushes Bearing Sulfonate Groups. Synthesis of polyelectrolyte brushes bearing sulfonate moieties was carried out using aqueous ATRP of the SPM monomer following our previously reported procedures[25,27,28] (Figure 1).

(26) Tiller, J. C.; Liao, C-J.; Lewis, K.; Klibanov, A. M. *P. Natl. Acad. Sci. U.S.A.* **2001**, *98*, 5981−5985.

(27) Jones, D. M.; Brown, A. A.; Huck, W. T. S. *Langmuir* **2002**, *18*, 1265−1269.

(28) Jones, D. M.; Huck, W. T. S. *Adv. Mater.* **2001**, *13*, 1256−1259.
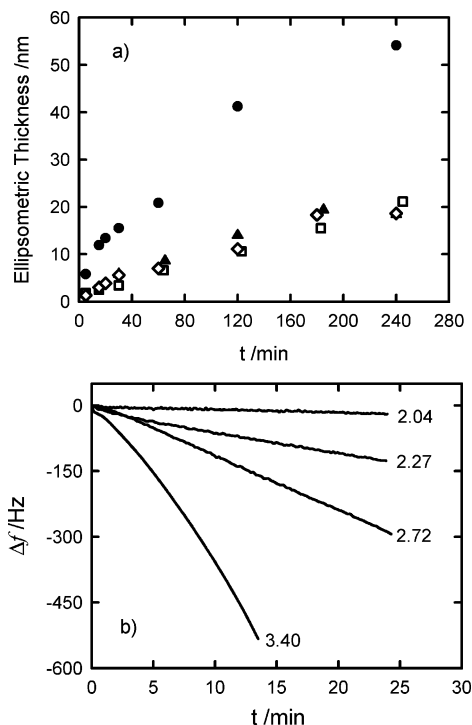
Figure 2. (a) Plot of ellipsometric polymer brush thickness versus polymerization time for polymerization solutions containing different Cu(I)/Cu(II) ratios: (□) 1.98, (▲) 2.04, (◆) 2.95, (●) 4.38. (b) Changes in frequency during SPM polymerization for solutions containing different Cu(I)/Cu(II) ratios. The ratios are indicated in the plot.

Briefly, the polymerization solution consisted of the Cu(I)/Bipy catalyst (promoting the activation), Cu(II)/Bipy deactivator (promoting capping), and the monomer (3-sulfopropylmethacrylate, potassium salt) in an aqueous methanolic solvent. The ratio between Cu(I) and Cu(II) thus determines the rate of polymerization and if, e.g., the Cu(I) concentration is increased, the reaction rate will increase as well. The aqueous environment leads to strongly accelerated polymerization leading to full conversion in minutes instead of hours or days. The substrates are left for a certain amount of time and then rinsed with water to yield smooth, covalently attached poly(3-sulfopropylmethacrylate) (PSPM, sulfonate) brushes up to several hundred nanometers in thickness. Figure 1 shows an atomic force image of 210 nm thick sulfonate brushes grown under well-controlled conditions on a Au substrate. The roughness is 1.45 nm measured over a scan size corresponding to $5 \times 5 \ \mu m^2$.

As we recently reported, the Cu(I)/Cu(II) ratio has a strong influence on the growth kinetics. Varying the Cu(I)/Cu(II) ratio in the polymerization solution between 2 and 3 did not show significant changes in the growth kinetics (~0.05 nm/min), as evidenced from the temporal evolution of brush thickness (*h*) (Figure 2). In our case, *h* was determined by ellipsometry and the measured value corresponds to the "dry" thickness of the polymer brush (it should be noted that these brushes are hygroscopic and will always contain some water). Increasing the Cu(I)/Cu(II) ratio above 4 resulted a significant increase in rate of polymerization, ~0.2 nm/min.

However, a more accurate description of the surface-initiated polymerization process can be obtained by following the kinetics with the QCM.[29] The QCM technique is extremely sensitive to slight changes in the mass coupled to the quartz crystal. QCM

(29) Moya, S. E.; Brown, A. A.; Azzaroni, O.; Huck, W. T. S. *Macromol. Rapid Comm.* **2005**, *26*, 1117−1121.
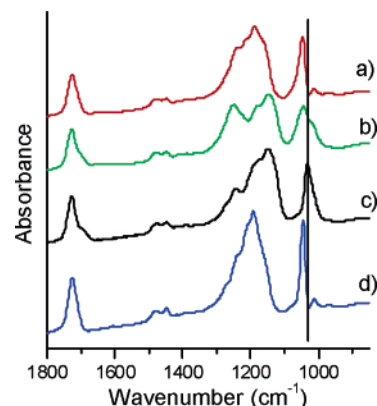
Figure 3. FTIR spectra of a (a) sulfonate brush soaked in 100 mM K⁺, (b) brush soaked in 100 mM Cu²⁺, (c) brush soaked in 100 mM Ag⁺, and (d) newly synthesized brush. The spectra show the stretching of carbonyl groups at 1730 cm⁻¹, CH₂ bending vibrations around 1450−1487 and 740 cm⁻¹, asymmetric sulfonate stretch around 1200 cm⁻¹, symmetric sulfonate stretching around 1045 cm⁻¹, and the stretching of C−O in the ester at 1245 cm⁻¹. The vertical line emphasizes the position of the symmetric stretching for the silver-loaded brush.

studies of the brush growth indicated detectable changes when varying the Cu(I)/Cu(II) ratio in the 2−3 range (Figure 3). Sulfonate brushes grown in polymerization solutions containing Cu(I)/Cu(II) ratios corresponding to 2.04, 2.27, and 2.72 showed an almost linear change in mass vs time, corresponding to 11.5, 87.6, and 218 ng/min·cm, respectively. It is important to note that this change in mass sensed by the quartz crystal is not solely associated to the addition of monomers units to the active polymer chains. The incorporation of solvent molecules into the brush layer is also sensed by the QCM.

As described above, samples did not show significant changes in ellipsometric thickness of the dry films while the QCM detected sensitive changes in the increasing mass. Assuming that the film density of the different "dry" films is nearly the same and similar to the density of the bulk polymer, we can say that the significant changes in mass as seen by QCM are mainly associated to different amounts of solvent incorporated into the brush layer. These results suggest that the molecular architecture of the polyelectrolyte brushes is strongly dependent on the polymerization rate.

Characterization of the SPM Brush. We further characterized the brush using FTIR, contact angle measurements, ellipsometry, and XPS. For these analyses we used thick sulfonate brushes (around 300 nm) in order to increase the accuracy in measurements of, e.g., contraction. The monomer used is in the form of a potassium salt, and hence, the synthesized polymer brush will have mainly potassium ions as counter ions. The large content of sulfonate groups in the polymer brush gives a highly hydrophilic surface with the capacity of uptake and exchange of metal ions. As shown in Figure 3, the association with different ions can be seen in FTIR spectra. Contact angle measurements of newly synthesized brushes showed advancing contact angles around 30°. Static and receding contact angles were difficult to estimate on the samples due to the almost complete wetting of the surface. Soaking of surfaces in Cu(II)- and Ag(I)-rich solutions significantly increased the contact angles measured on the surfaces. Overnight soaking of 100 mM K(I), Cu(II), and Ag(I) increased advancing contact angles from 29°, 39°, and 31° to 34°, 48°, and 51°, respectively. However, measurements of surface energy using contact angles assume that the surface does not interact with the water drop, and in our case, this is not true. Despite this, the increase in contact angles shows that when the sulfonate

Table 1. Concentration of Different Components (in at %) at the Surface of Sulfonate Brush as a Consequence of Soaking in Water, Soaking Overnight in 100 mM Metal Ion Solution, or Ag(I) Loading Using Different Ag(I) Concentrations[a]

	Na	Cu(II)	Cu(I)	Ag	K	O sum	NH	N	C sum	S	Me+/S[b]	N(tot)/Cu(tot)	Ag/S	time (h)
H$_2$O 112 h	2.4		0.2		1.9	29.9		0.9	58.7	6.0	0.7	4.0		112
H$_2$O 24 h	2.4		0.3		3.5	30.4		0.8	56.2	6.2	1.0	2.7		24
reference		0.1	0.3		5.3	30.7		1.2	57.0	5.5	1.1	3.2		
Cu overnight		3.1	0.3			31.1	0.8	0.8	58.3	5.8	1.1	0.5		
K overnight	0.7				7.6	34.6			54.6	5.8	1.4			
Ag overnight				10.4		29.2			54.7	5.6	1.9		1.9	
1 μM 27 h	3.9	0.1	0.3		2.0	29.7		1.2	56.9	6.0	1.1	2.9		27
1 μM 30 h	1.3	0.4	0.3	0.1	0.8	28.0		2.7	61.2	5.3	0.6	4.0		30
10 μM	1.6	0.4	0.3	0.3	0.8	28.1		2.3	60.9	5.4	0.7	3.4		30
100 μM	0.8	0.2	0.3	2.7	1.0	28.0		2.0	59.4	5.6	0.9	4.0	0.5	30
1 mM	0.4	0.1	0.2	4.2		29.2		1.2	59.1	5.7	0.9	4.1	0.7	30
10 mM				9.7		28.5			56.4	5.5	1.8		1.8	30
50 mM				7.5		30.8			55.2	6.6	1.1		1.1	24
100 mM				14.5		27.9			52.9	4.7	3.1		3.1	30
100 mM				7.4		31.2			54.9	6.6	1.1		1.1	24
200 mM				6.7		31.2			55.7	6.5	1.0		1.0	24
500 mM				7.0		31.4			55.0	6.5	1.1		1.1	24
700 mM				7.4		31.4			54.8	6.4	1.2		1.2	24
1 M				7.0		31.1			55.6	6.3	1.1		1.1	24

[a] Reference sample represents brush after synthesis. [b] Me+/S = ratio between positive charges from metal ions and amount of sulfur, i.e., sulfonate groups.

groups become coordinated to metal ions, the total charge of the surface decreases, thus resulting in a somewhat lower hydrophilicity.

We performed XPS analysis on sulfonate brushes to determine the nature and amount of metal ions present in these brushes. For the as-synthesized brushes, we find, apart from K$^+$, small quantities of copper from the catalyst (Table 1), similar to what has been found for poly(triphenylamine acrylate) brushes.[30]

Cu is present in the synthesis in the form of a Cu(BiPy)$_2$ complex[31−32] and possibly also in the form of a Cu^{II}(BiPy) complex.[33] XPS analyses showed that Cu is taken up by the brush both as Cu(I) and Cu(II). The ratio between Cu and N ($\sim$1:4 (Table 1)) suggests that copper is taken up as Cu(BiPy)$_2$ complexes. Furthermore, this ratio suggests that copper coordinates both two bipyridyl molecules and a sulfonate group inside the brush. This represents a type of interaction that has previously been suggested by Mitchell[34] in complexes between Cu(II) bipyridyl and 3-(trimethylsilyl)propanesulphonate. Moreover, the presence of BiPy ligands explains the uptake into neutral brushes observed previously.[30] Another possibility for Cu to be trapped inside the brush would be through formation of organometallic centers (as discussed by, e.g., Matyjaszewski[19]). However, when the newly synthesized brush was soaked in solutions of, e.g., 100 mM K$^+$ or Ag$^+$, all Cu(I/II) ions inside the brush were replaced by ions from solution (Table 1). The disappearance of copper as a consequence of the soaking shows that no organometallic centers are formed in the brush during the polymerization but that the copper in the brush is in an easily exchangeable form. Furthermore, the presence of the BiPy ligand inside the brush explains the stability of Cu(I) inside the brush. Since the copper is easily removed from the brush, it is not expected to cause problems in practical applications using the sulfonate brush.

Bond formation between the sulfonate group and metal ions can be studied using FTIR. The coordination geometry formed splits the asymmetric sulfonate stretching vibration ($\sigma_{as}(SO_3)$)

in FTIR spectra (around 1200 cm^{-1}, Figure 3). This indicates that the bond formation between the metal ion and the sulfonate removes the double degeneracy of the otherwise symmetric (C_{3v}) sulfonate group[35] and, thus, that the cations are asymmetrically bound to the sulfonate groups. The shape and intensity of the different compounds in $\sigma_{as}(SO_3)$ together with the position of the symmetric vibration ($\sigma_{sym}(SO_3)$) can give information about which cation is bound to the sulfonate group, and furthermore, $\sigma_{as}(SO_3)$ can also give some indications about hydration of the sulfonate groups.[35] As a consequence of soaking in metal-ion-rich solutions, the $\sigma_{as}(SO_3)$ peak changed shape with all cations used (Figure 3) and $\sigma_{sym}(SO_3)$ was shifted downward in wavenumber (to 1035 cm^{-1}) after loading the brush with silver ions.

Loading of the SPM Brush with Silver. It is well-known that polyelectrolyte brushes "collapse" in contact with salt solutions. For thick polyelectrolyte brushes, this uptake of silver and the subsequent brush collapse was visible to the eye in the form of color changes (interference colors) in the dried samples. These changes in color and thus variation in thickness are shown in Figure 4. From these changes we could conclude that for lower concentrations of silver (1 mM), the diffusion into the brush took up to 24 h, while for higher concentrations (100 mM), the uptake was more rapid. The difference in final contraction between the 1 mM loaded brush and 100 mM is due to the brush not yet being "saturated" with silver ions at 1 mM; thus, it does not contract to the same extent. The slight difference in color in the images after 23 h represents $\sim$3 nm in dry thickness. This difference is smaller than the differences in thicknesses across the measured area of the film ($\sim$5−15 nm difference) and, thus, not significant. For the sample soaked in 1 mM, the contraction represents a total decrease in dry thickness (measured by ellipsometer) from 330 to 276 nm and, for the 100 mM sample, 331 to 233 nm.

From XPS data it can be seen that immersion into 1 mM silver solution replaced all potassium ions at the surface of the brush film (Table 1) while 10 mM Ag$^+$ ions were needed to replace Na$^+$ (present as a contamination due to the high ion exchange capacity of the brush) and Cu^{2+} ions. The samples loaded for 30 h had a larger Ag/S ratio than the ones soaked for 24 h. The

(30) Whiting, G. L.; Snaith, H. J.; Khodabakhsh, S.; Andreasen, J. W.; Breiby, D. W.; Nielsen, M. M.; Greenham, N. C.; Friend, R. H.; Huck, W. T. S. *Nano. Lett.* **2006**, *6*, 573−578.

(31) Matyjaszewski, K. *Macromolecules* **1999**, *32*, 9051−9053.

(32) Matyjaszewski, K.; Nanda, A. K.; Tang, W. *Macromolecules* **2005**, *38*, 2015−2018.

(33) Gustafson, R. L.; Martell, A. E. *J. Am. Chem. Soc.* **1959**, *81*, 525−529.

(34) Mitchell, P. R. *Dalton. Trans.* **1979**, 771−776.

(35) Zundel, G. *J. Membr. Sci.* **1982**, *11*, 249−274.
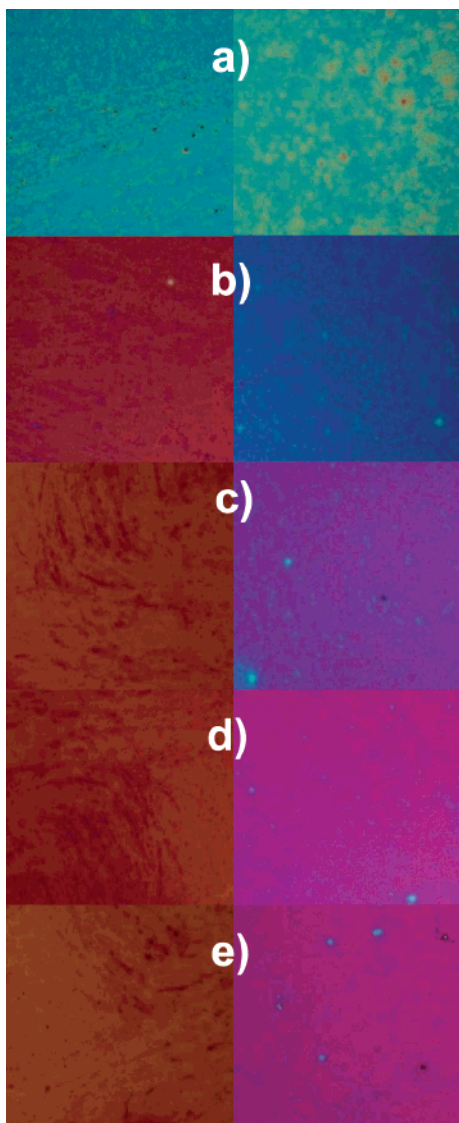
Figure 4. Changes in interference color of the polyelectrolyte brush with time. The right images show sample soaked in 1 mM Ag$^+$ and the left ones in 100 mM Ag$^+$. (a) Initially, (b) 5 h, (c) 23 h, (d) 30 h, and (e) 106 h. The size of the small images in the panel represents $77 \times 77 \ \mu m^2$ for the right column and $144 \times 144 \ \mu m^2$ for the left column.

explanation for this is that a more careful rinsing was preformed for the samples after 24 h and, thus, these samples have lost excess electrolyte from the solution that was trapped inside the collapsed brush.

At 10 mM silver, the surface starts to be saturated with silver leading to a Ag/S ratio of more than 1 (Table 1). From FTIR data (Figure 5) it can be seen that at this concentration the sulfonate groups in the bulk of the brush are partly coordinated to silver ions, i.e., the symmetric sulfonate vibration is shifted downward. However, the final peak position for a saturated sulfonate brush is found at concentrations of 50 mM Ag and higher. Thus, thick brushes (around 300 nm) should be soaked in at least 50 mM silver solution to fully load the brush with silver ions.

Antibacterial Properties. To create a surface with antibacterial properties, it is desirable that the surface is toxic to bacteria at contact to hinder attachment, colonization, and growth. To study this, sulfonate brushes with and without silver were sprayed with gram positive (*S. aureus*) and gram negative bacteria (*P. aeruginosa*) and inoculated overnight. These studies show that bacterial growth and formation of a biofilm take place as "normal"
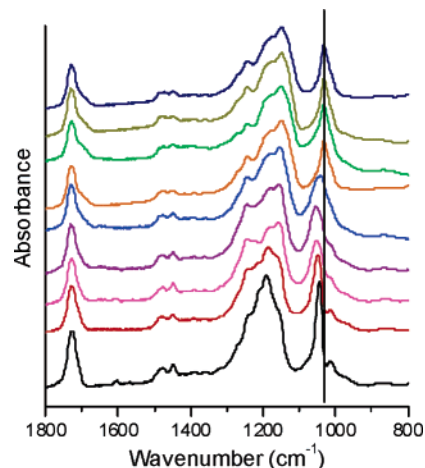
Figure 5. Change in sulfonate symmetrical stretching as a consequence of silver loading. The curves represent brushes loaded with (from the top) 1 M, 500 mM, 100 mM, 50 mM, 10 mM, 1 mM, 100 μM, H$_2$O, and brush as synthesized. The vertical line shows the position of symmetric sulfonate stretch for sulfonate coordinated to silver ions.
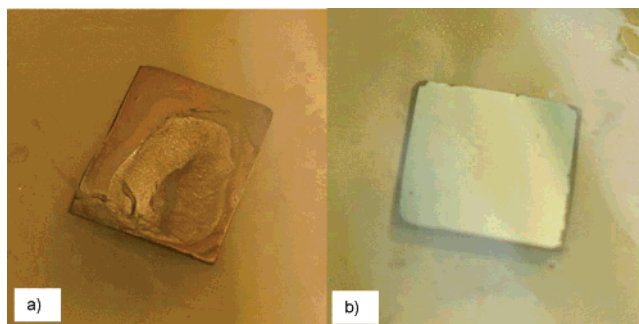
Figure 6. (a) Growth of *S. aureus* on a piece of silica wafer covered with sulfonate brush. (b) Absence of growth of *S. aureus* on a silica wafer covered with silver-loaded sulfonate brushes. Both images represent wafer pieces positioned in a petri dish and covered with growth agar.

on sulfonate brushes but is completely inhibited on silver-loaded brushes (Figure 6) for both bacteria.

Leaching of Silver from a Silver-Loaded SPM Brush. For an antibacterial surface, slow leaching of silver ions from the film is also desired in order to prevent bacterial growth in the vicinity of the surface (zone of inhibition). Furthermore, it is interesting to know how this leaching occurs with time and how the leaching is affected by solution composition. In order to test this, leaching experiments were performed in distilled water, in physiological solution (150 mM NaCl), and in 150 mM NaNO$_3$ using thick (initial thickness of around 300 nm) silver-loaded brushes.

It has previously been described that collapsing polyelectrolyte brushes can trap excess electrolyte ions inside the brush than subsequently can be leached out. When sulfonate brushes collapsed in, e.g., 100 mM AgNO$_3$, the uptake of silver per sulponate group was higher than 1:1 (Table 1), suggesting entrapment of electrolyte from solution inside the brush. Repeated immersion of these brushes into 5 mL aliquots of distilled water showed continuous release of silver as a function of volume, while the silver concentration at the surface of the samples changed very little (Figure 7a and d). A diffusion of excess electrolyte from the inner parts of the brush layer toward the surface can explain why silver is not depleted at the surface of the brush during the 6 h that the experiment lasted. The highest silver
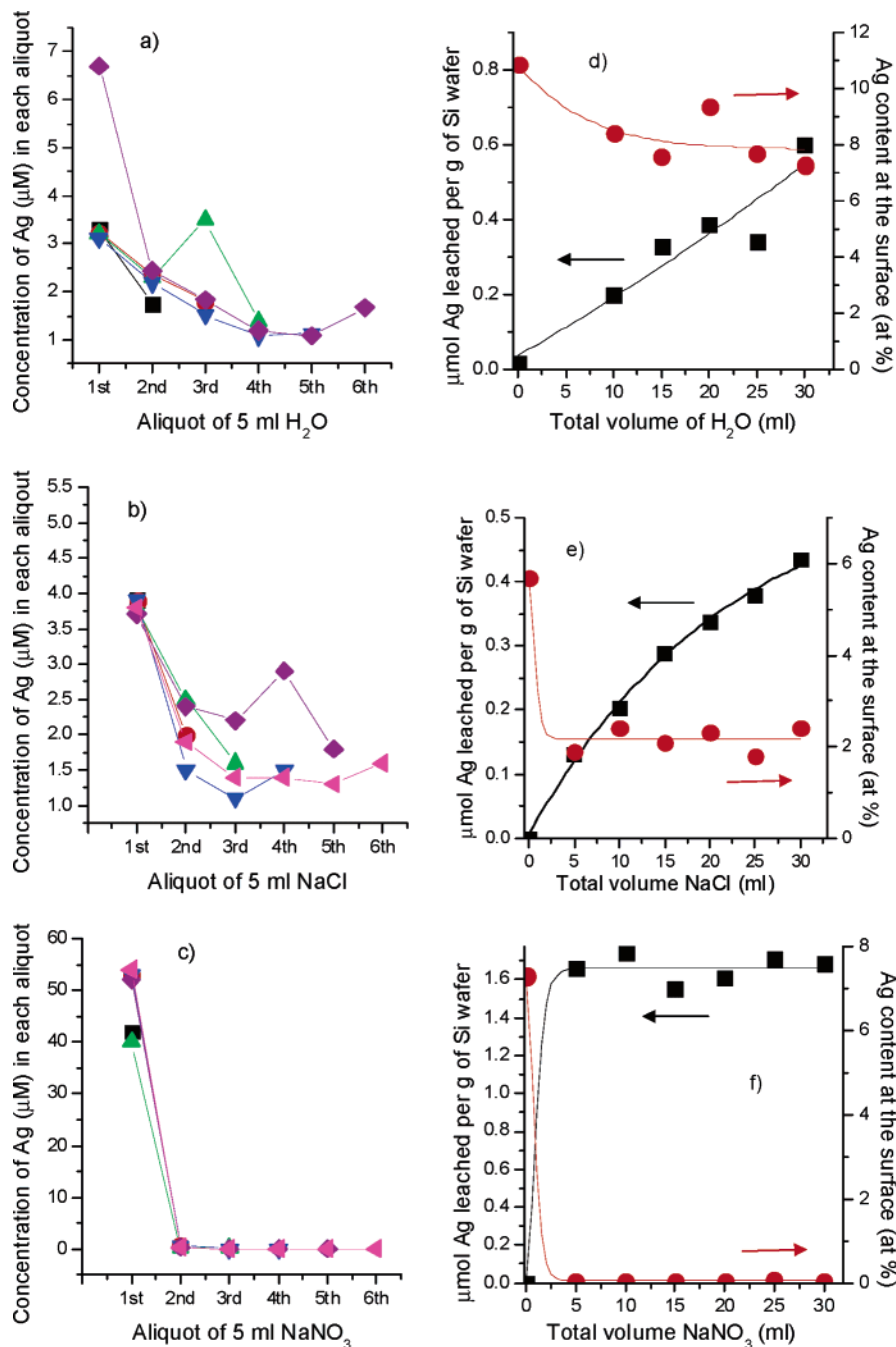
Figure 7. (a−c) Silver concentration in solution after leaching into 5 mL aliquots of (a) distilled water, (b) 150 mM NaCl, and (c) 150 mM NaNO₃. The different lines and symbols represent different samples, and the individual data points represent the Ag concentration in each aliquot. (d−f) Total amount of silver (■ μmol/g Si wafer) leached from the surface of each sample and remaining silver concentration at the surface (● at %), for leaching into (d) distilled water, (e) NaCl, and (f) NaNO₃. The lines in (d−f) are only a guide for the eye. Slight difference in rinsing between the sample sets presented in (a) and (d) compared to (b), (e), (c), and (f) gives rise to the increased amount of Ag at the surface at $t = 0$ in (d) compared to (e) and (f) (as discussed in the text).

release was found in the first aliquots, and with continued "rinsing" the silver concentration in the aliquots decreased (Figure 7a).

A similar behavior was seen if the silver-loaded brush was immersed into NaCl solution. The first aliquots contained the most silver, and with rinsing, the concentration decreased in the aliqouts. However, there was a larger difference between different samples in the experiment using NaCl (Figure 7b). If the silver-loaded brush was immersed into NaNO₃, all the silver ions were released into the first aliquot (Figure 7c).

Since the brush displays high cationic exchange capabilities, a displacement of silver ions with sodium ions can be expected

when NaNO₃ was used, and this is further illustrated by the loss of silver at the surface (Figure 7f). The same result should be obtained when using NaCl, but here silver can still be detected in fairly high amounts at the surface (Figure 7e). The answer to why silver remains lies in the strong interaction between silver and chloride. When the silver-loaded brush is immersed into NaCl, silver ions from the brush form a AgCl(s) precipitate inside the brush. The presence of this particulate phase gives the brush a grainy appearance that could also be seen in optical microscope (Figure 8) or by the eye as "cloudiness" at the surface. The identity of this precipitate was also confirmed using XRD, which
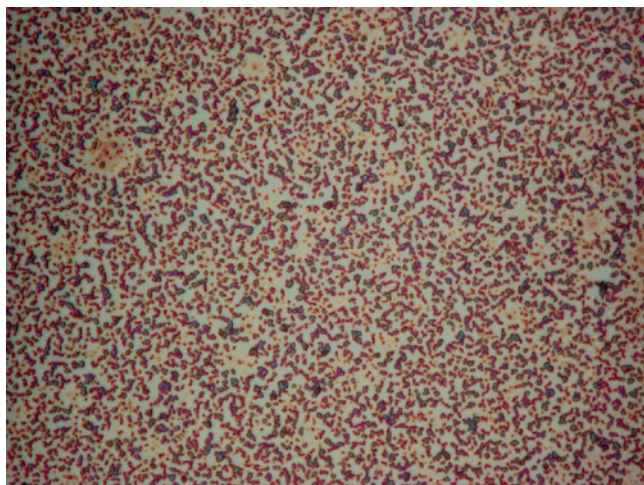
Figure 8. Optical microscopy image of brush with AgCl(s) particles. The size of the image is 107×80 μm^2.

Figure 9. Sulfonate stretching vibration for (from the top) a Ag-loaded brush leached into 25 mL of $NaNO_3$, 15 mL of $NaNO_3$, 5 mL of $NaNO_3$, 30 mL of NaCl, 15 mL of NaCl, 5 mL of NaCl, 30 mL of H_2O, 15 mL of H_2O, a Ag-loaded brush, and a brush as synthesized. The position of the symmetric stretching (around 1050 cm^{-1}) shows exchange between Ag^+ and Na^+ in the Ag-loaded brush leached into NaCl or $NaNO_3$. The position of the symmetric stretching for silver-loaded brushes is shown with a vertical line. The sulfonate groups in the brush leached into water maintains Ag^+ as counterion, as shown in the sketches on the right-hand side of the figure.

showed small broad peaks at *d* values 3.22, 2.77, 1.96, 1.67, and 1.60 Å, coinciding with reflections from AgCl(s).[36] The reason for the continued leaching of silver into NaCl solution is due to formation of soluble silver chloride complexes such as $AgCl_2^-$ and/or $AgCl_3^{2-}$ from the AgCl(s) particulate phase.[37]

To obtain information about the inner part of the brush layer FTIR was used. Spectra of silver-loaded brushes leached with $NaNO_3$ or NaCl show that sodium ions coordinate the sulfonate moieties inside the brush (Figure 9). This indicates that all silver ions have been exchanged for sodium ions in both solutions. However, if the brush is immersed in water, no such change could be seen, and FTIR indicated that silver was still coordinated to the sulfonate moieties. Thus, we can conclude that when silver was leached into water, the main part of the silver came from excess silver ions trapped within the brush. The exchange to a sodium-loaded brush was found to be reversible, and thus, if the brush was re-immersed into silver nitrate solution, the Na ions again got replaced by Ag ions. In brushes containing AgCl(s) precipitate, this meant an increase in total silver content (Ag^+ + AgCl(s)) compared to brushes loaded with silver ions only once.

A large constituent of body fluids is NaCl and thus, if a silver-loaded brush got in contact with body fluids or other physiological solutions we can hypothesise that all or parts of the silver present in the brush would be transformed into AgCl(s). However, this salt was also shown to leach silver into NaCl solutions and can thus be expected to work in a similar way as a brush with silver ions. Furthermore, due to the good ion-exchange properties of the brush, one can envisage reloading of the brush with silver ion once it is depleted or further increase the silver content by re-immersing a AgCl(s) containing brush into Ag^+ solution.

When the samples were leached into water or into NaCl solution, the amount of silver at the surface only slowly decreased as a function of volume. Even after six 1 h washings of 5 mL of solution, silver still remains at the surface (8 at % in water and 2 at % in NaCl solution). This indicates that these surfaces maintain silver and display a long-term leaching effect, two factors highly desirable for these types of devices. The total exchange seen in $NaNO_3$ shows that the samples used here contained $\sim$1.6 μmol of Ag per g of Si wafer. After 6 h of leaching into water or NaCl, only 0.4−0.6 μmol of Ag had leached out per g of Si wafer. Thus, it can be expected that the antibacterial effect remains for a much longer period of time. However, the leaching from these films is of course a function of fluid volume and throughput. Since 1 h of equilibrium time was enough to completely exchange the silver in $NaNO_3$, we assume that the most important leaching variables in this system are connected to the volume of solution used.

Conclusions

Sulfonate polyelectrolyte brushes could be grown in a controlled manner using ATRP to give brush thicknesses ranging from a few nanometers to several hundred nanometers. The brushes were highly hydrophilic and functioned very well as cation exchangers. When the brushes were loaded with silver ions it was shown that they inhibited growth of both gram positive and gram negative bacteria. Furthermore, the silver-loaded brushes were able to maintain silver at the surface during leaching and also showed slow leaching of silver ions in water and in NaCl medium. Thus, silver-loaded sulfonate brushes exhibit properties highly desirable for antibacterial surfaces. We envisage that polyelectrolyte brushes can be used as a general platform to create antibacterial surfaces by exploiting the supramolecular chemistry of ion-exchange reactions.

(36) Sathiyanarayanan, S.; Sahre, M.; Kautek, W. *Electrochim. Acta* **1998**, *43*, 2985−2989.
(37) Gammons, C. H.; Yu, Y. *Chem. Geol.* **1997**, *137*, 155−173.